

9. DATA REPORT: MAGNETIC PROPERTIES OF ODP LEG 191 SITE 1179 SEDIMENTS¹

Benjamin C. Horner-Johnson² and William W. Sager³

INTRODUCTION

As reported by Shipboard Scientific Party (2001b) in the Site 1179 chapter of the *Initial Reports* volume, Leg 191 Site 1179 is located on abyssal seafloor northwest of Shatsky Rise, ~1650 km east of Japan. This part of the Pacific plate was formed during the Early Cretaceous, as shown by northeast-trending M-series magnetic lineations that become younger toward the northwest (Larson and Chase, 1972; Sager et al., 1988; Nakanishi et al., 1989). The site is situated on magnetic Anomaly M8 (Nakanishi et al., 1999), corresponding to an age of ~129 Ma and the Hauterivian stage of the Early Cretaceous (Gradstein et al., 1994, 1995).

The sediments recovered at Site 1179 are split into four lithostratigraphic units based on composition and color (Shipboard Scientific Party, 2001b). Unit I (0–221.52 meters below seafloor [mbsf]) is a dominantly olive-gray clay- and radiolarian-bearing diatom ooze. Unit II (221.52–246.0 mbsf) is a yellowish brown to light brown clay-rich and diatom-bearing radiolarian ooze. Unit III (246.0–283.53 mbsf) is composed of brown pelagic clay. Unit IV (283.53–377.15 mbsf) is composed of chert and some porcellanite; any softer sediments present were washed out of the core barrel by the fluid circulating during the coring process.

SAMPLING

The working halves of the cores containing Units I, II, and III were sampled for paleomagnetic analyses using a tool shaped for standard Japanese paleomagnetic “cubes” (octagonal horizontal section; faces

¹Horner-Johnson, B.C., and Sager, W.W., 2004. Data report: Magnetic properties of ODP Leg 191 Site 1179 sediments. In Sager, W.W., Kanazawa, T., and Escutia, C. (Eds.), *Proc. ODP, Sci. Results*, 191, 1–19 [Online]. Available from World Wide Web: <http://www-odp.tamu.edu/publications/191_SR/VOLUME/CHAPTERS/008.PDF>. [Cited YYYY-MM-DD]

²Department of Earth Science, Rice University, 6100 South Main Street, Houston TX 77005-1892, USA.

ben@esci.rice.edu

³Department of Oceanography, Texas A&M University, College Station TX 77843-3146, USA.

parallel to a 2-cm square are 1.5 cm wide; missing 0.25 cm at each corner of the square). The sediment samples were placed in standard ODP sample cubes (2 cm × 2 cm × 2 cm), but instead of a sample volume of 8 cm³, these were missing ~0.0625 cm³ from each corner, for a total sample volume of 7.75 cm³. The standard ODP magnetic direction conventions were used: the x-axis of the sample is positive downward from the split face of the working half of the core; the y-axis is positive to the right when looking upcore and parallel to the split face of the core; the z-axis is positive downcore and parallel to the split face of the core. Sample cubes are marked with an arrow that points upcore (-z).

Every core was sampled at an average sampling rate of one sample per 0.75 m of core available for sampling. Each identified magnetic anomaly was sampled at least once. All of the samples were measured for natural remanent magnetization (NRM) and were alternating-field (AF) demagnetized by steps of 5, 10, 15, 20, 25, 30, 35, 40, 50, 60, and 70 mT. Inclination, declination, and maximum angular deviation were determined from principal component analysis of Zijderveld plots of the discrete sample AF-demagnetization measurements. These analyses were carried out on the ship and the data are accessible through the Janus database.

ISOTHERMAL REMANENT MAGNETIZATION

Method

Isothermal remanent magnetization (IRM) analysis of 77 selected samples was done on the ship using an Analysis Services Company impulse magnetizer model IM-10, which is capable of applying magnetic fields from 0.02 to 1.35 T. We used the impulse magnetizer to impart a series of remanent magnetizations on a sample in steps of 25, 50, 75, 100, 200, 300, 400, 500, 750, and 1000 mT (Table T1). For seven samples of Core 191-1179C-25X the impulse series was 25, 50, 100, 150, 200, 300, 400, 500, 750, and 1000 mT (Table T1). At each step, the magnetic intensity of each sample was measured on the 2G Enterprises pass-through cryogenic magnetometer.

T1. IRM intensities, p. 13.

Results

We analyzed 28 samples from Lithostratigraphic Unit I in Cores 191-1179C-1H, 2H, 9H, 12H, and 19H, ranging in depth from 1.30 to 219.68 mbsf. The measured magnetic intensities range from a minimum of 0.00658 A/m for Sample 191-1179C-19H-2, 38–40 cm (25-mT impulse field), to a maximum of 13.160 A/m for Sample 9H-4, 38–40 cm (750-mT impulse field) (Table T1). The magnetic intensities reported in Table T1 for samples from Cores 191-1179C-12H and 19H are ~50% of the true values, due to an error in placement of the discrete sample tray; the samples were 10 cm from the center of the 30-cm measuring width of the pass-through cryogenic magnetometer, but 85% of the input comes from within 20 cm of the central measuring point (Shipboard Scientific Party, 2001a).

IRM analyses were run on 23 samples from Lithostratigraphic Unit II in Cores 191-1179C-20H, 21H, and 22H, ranging from 229.44 to 243.68 mbsf. The measured magnetic intensities range from a minimum of 0.7059 A/m for Sample 191-1179C-21H-1, 68–70 cm (25-mT impulse

field), to a maximum of 6.2634 A/m for Sample 22H-1, 48–50 cm (750-mT impulse field).

For lithostratigraphic Unit III, 26 samples from Cores 191-1179C-22H, 25X, and 26X were analyzed. The depth range of the samples was from 247.64 to 283.29 mbsf, and the magnetic intensities range from a minimum of 1.9544 A/m for Sample 191-1179C-22H-6, 134–136 cm, to a maximum of 28.645 A/m for Sample 26X-CC, 10–12 cm.

For all 77 of the samples analyzed for IRM, the magnetization carrier was determined to be magnetite.

ANISOTROPY OF ANHYSTERETIC REMANENT MAGNETIZATION

Method

We analyzed samples from Lithostratigraphic Units I, II, and III for anisotropy of anhysteretic remanent magnetization (AARM) at the Institute for Rock Magnetism at the University of Minnesota (USA). We selected 25 samples from Unit I, roughly every 12.5 mbsf, from Cores 191-1179B-1H through 3H, 5H, and 6H and Cores 191-1179C-3H, 4H, 6H–8H, 10H–13H, and 15H–20H. We selected 3 samples from Cores 191-1179C-20H and 21H in Unit II and 9 samples from Cores 191-1179C-22H, 23H, 25X, and 26X in Unit III.

An AF applied with a D-Tech AF demagnetizer on each of the x-, y-, and z-axes cleaned each sample of any remanence softer than 200 mT. Next, the NRM of each sample was measured with a 2G Superconducting Rock Magnetometer (SRM) (Table T2).

An anhysteretic remanent magnetization (ARM) of 100 mT with a superimposed 100- μ T direct-current bias was added to the x-axis of the sample with a Schonstedt magnetizer. For the Schonstedt magnetizer, the decay rate of the AF field is 2.5 mT per half-cycle. The sample was measured again with the SRM, and then the x-axis was cleaned with a 200-mT AF applied with the D-Tech AF demagnetizer. The process was repeated for the y- and z-axes (Table T2).

Results

The term anisotropy of anhysteretic remanent magnetization implies the determination of the second-rank tensor defining an ellipsoid. This is done by measuring the NRM and ARM for 15 different sample orientations. Our sample cubes were too large to fit into the available rigs for applying the 100-mT ARM to the 12 orientations not normal to the faces of the sample cubes. Instead, we used the difference between the ARM and the NRM for each axis to calculate a measure of the anisotropy of the ARM:

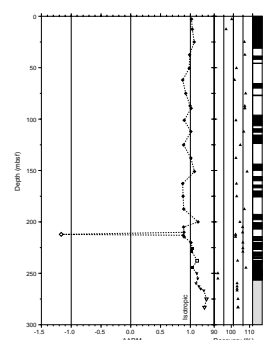
$$\text{AARM} = \frac{1}{2} \{[(\text{ARM}_x - \text{NRM}_x) + (\text{ARM}_y - \text{NRM}_y)] / (\text{ARM}_z - \text{NRM}_z)\}.$$

The results of the AARM calculations in Table T2 are shown in Figure F1. Some of the samples had previously been tested using IRM, and the IRM acquired in the maximum applied field (1 T) was too high to be completely cleaned before the AARM tests.

Sedimentary magnetic records may be affected by inclination shallowing if the weight of the upper layers of sediment causes lower layers

T2. Anisotropy of AARM, p. 15.

F1. AARM vs. depth, p. 7.



to compress and the magnetic particles to rotate to a shallower inclination with the other compressed sediment grains. Figure F1 shows that the core recovery was almost always >100% and that AARM does not correlate with core recovery.

For the Unit I samples, the AARM values fluctuate between 0.871 and 1.129 with no clear depth progression. Both the Unit II and Unit III samples have AARM values >1.0, with the largest values indicating larger possible inclination shallowing, increasing with depth in Unit III.

ANISOTROPY OF MAGNETIC SUSCEPTIBILITY

Method

The anisotropy of magnetic susceptibility (AMS) for each sample was calculated by inserting the sample into a Geofyzika Brno KLY_2 Kappa-Bridge alternating-current (AC) susceptibility bridge in 15 different orientations. The software provided by Geofyzika Brno determined the anisotropy tensor from the measurements. Table T3 lists the depth, F -statistics for anisotropy of magnetic susceptibility (Fig. F2), declinations and inclinations of the maximum, intermediate, and minimum axes of the AMS ellipsoid (Fig. F3) and their 95% confidence angles (Figs. F4 and F5), the mean magnetic susceptibility, the normed principal susceptibilities and their uncertainties, the components of the anisotropy of magnetic susceptibility tensor, and measures of anisotropy based on those principal susceptibilities.

Results

AMS was determined for 51 samples from Unit I, 20 samples from Unit II, and 15 samples from Unit III. In Unit I, 42 of the 51 samples have significantly anisotropic AMS ellipsoids ($F > 3.84$). Of the 42 anisotropic samples, there are 25 significantly prolate/triaxial AMS ellipsoids ($F_{12} > 4.25$), 30 significantly oblate/triaxial AMS ellipsoids ($F_{23} > 4.25$), and 2 AMS ellipsoids that are neither significantly prolate/triaxial nor significantly oblate/triaxial (Samples 191-1179C-5H-6, 38–40 cm, and 17H-4, 120–122 cm). There are 15 triaxial AMS ellipsoids, 10 prolate AMS ellipsoids, and 15 oblate AMS ellipsoids.

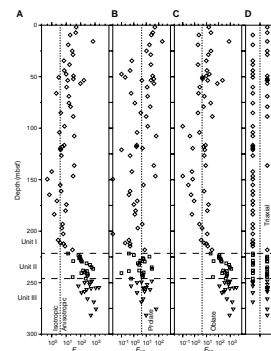
In Unit II, all 20 samples are significantly anisotropic and significantly oblate/triaxial. Half of the samples are significantly prolate/triaxial, which means there are 10 triaxial AMS ellipsoids and 10 oblate AMS ellipsoids. In Unit III, all 15 samples are significantly anisotropic and significantly oblate/triaxial. Ten of the samples are also significantly prolate/triaxial, so there are 10 triaxial AMS ellipsoids and 5 oblate AMS ellipsoids.

The measures of anisotropy defined and listed in Table T3 are shown vs. depth below seafloor in Figure F6. There is a shift in AMS ellipsoid shape (T, q) from approximately equal distributions of prolate and oblate in sedimentary Unit I to dominantly oblate ellipsoids in sedimentary Units II and III (Fig. F6A, F6B).

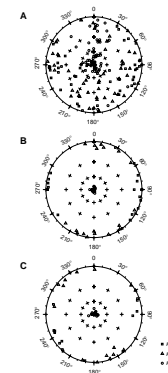
The measure of anisotropy L (Fig. F6C; Table T2) is very close to isotropic for Units I, II, and III. The other measures of anisotropy (F, P , and P_j) shown in Figures F6D–F6F are all close to isotropic in Unit I and more anisotropic in Units II and III. There is an increase in anisotropy beginning with Core 191-1179C-21H (229.3 mbsf).

T3. AMS, p. 16.

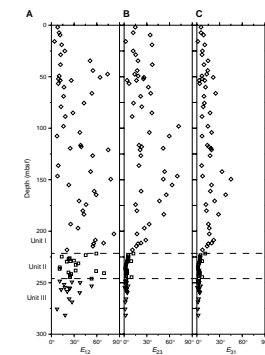
F2. F -statistics for anisotropy, p. 8.



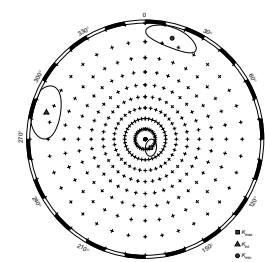
F3. Principal axes of AMS ellipsoids, p. 9.



F4. Variation in 95% confidence angles, p. 10.



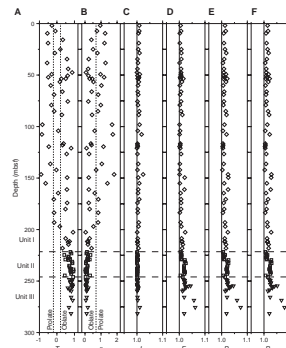
F5. Principal axes of the triaxial AMS ellipsoid, p. 11.



ACKNOWLEDGMENTS

This research used samples provided by the Ocean Drilling Program (ODP). ODP is sponsored by the U.S. National Science Foundation (NSF) and participating countries under management of Joint Oceanographic Institutions (JOI), Inc. We thank Mike Jackson and the rest of the staff at the Institute for Rock Magnetism at the University of Minnesota for the use of their KappaBridge and other magnetism equipment on which some of this research was done during a longer-than-normal informal visit. We also thank JOI/U.S. Science Support Program for funding the postcruise portion of this research and the trip to the Institute for Rock Magnetism (grant number F001323). In addition, the comments of two reviewers were very helpful for getting this data report into shape for publication.

F6. Anisotropy measures, p. 12.



REFERENCES

- Gradstein, F.M., Agterberg, F.P., Ogg, J.G., Hardenbol, J., van Veen, P., Thierry, J., and Huang, Z., 1994. A Mesozoic time scale. *J. Geophys. Res.*, 99:24051–24074.
- Gradstein, F.M., Agterberg, F.P., Ogg, J.G., Hardenbol, J., van Veen, P., Thierry, J., and Huang, Z., 1995. A Triassic, Jurassic and Cretaceous time scale. In Berggren, W.A., Kent, D.V., Aubry, M.P., and Hardenbol, J. (Eds.), *Geochronology, Time Scales and Global Stratigraphic Correlation*. Spec. Publ.—SEPM (Soc. Sediment. Geol.), 54:95–126.
- Larson, R.L., and Chase, C.G., 1972. Late Mesozoic evolution of the western Pacific Ocean. *Geol. Soc. Am. Bull.*, 83:3627–3643.
- Nakanishi, M., Sager, W.W., and Klaus, A., 1999. Magnetic lineations within Shatsky Rise, northwest Pacific Ocean: implications for hot spot–triple junction interaction and oceanic plateau formation. *J. Geophys. Res.*, 104:7539–7556.
- Nakanishi, M., Tamaki, K., and Kobayashi, K., 1989. Mesozoic magnetic anomaly lineations and seafloor spreading history of the northwestern Pacific. *J. Geophys. Res.*, 94:15437–15462.
- Sager, W.W., and Pringle, M.S., 1988. Mid-Cretaceous to early Tertiary Apparent Polar Wander Path of the Pacific plate. *J. Geophys. Res.*, 93:11753–11771.
- Shipboard Scientific Party, 2001a. Explanatory notes. In Kanazawa, T., Sager, W.W., Escutia, C., et al., *Proc. ODP, Init. Repts.*, 191, 1–49 [CD-ROM]. Available from: Ocean Drilling Program, Texas A&M University, College Station TX 77845-9547, USA.
- Shipboard Scientific Party, 2001b. Site 1179. In Kanazawa, T., Sager, W.W., Escutia, C., et al., *Proc. ODP, Init. Repts.*, 191, 1–159 [CD-ROM]. Available from: Ocean Drilling Program, Texas A&M University, College Station TX 77845-9547, USA.

Figure F1. Anisotropy of Anhysteretic Remanent Magnetization (AARM) vs. depth for samples in sedimentary Units I, II, and III. Open symbols = samples that previously had acquired an IRM in a 1-T applied field and were unable to be completely cleaned before AARM analysis. The right part of the figure shows the core recovery percentage (inverted triangles) and the magnetic polarity of the sediments (black = normal polarity, white = reversed polarity, gray = anomalies not identified) (Shipboard Scientific Party, 2001b).

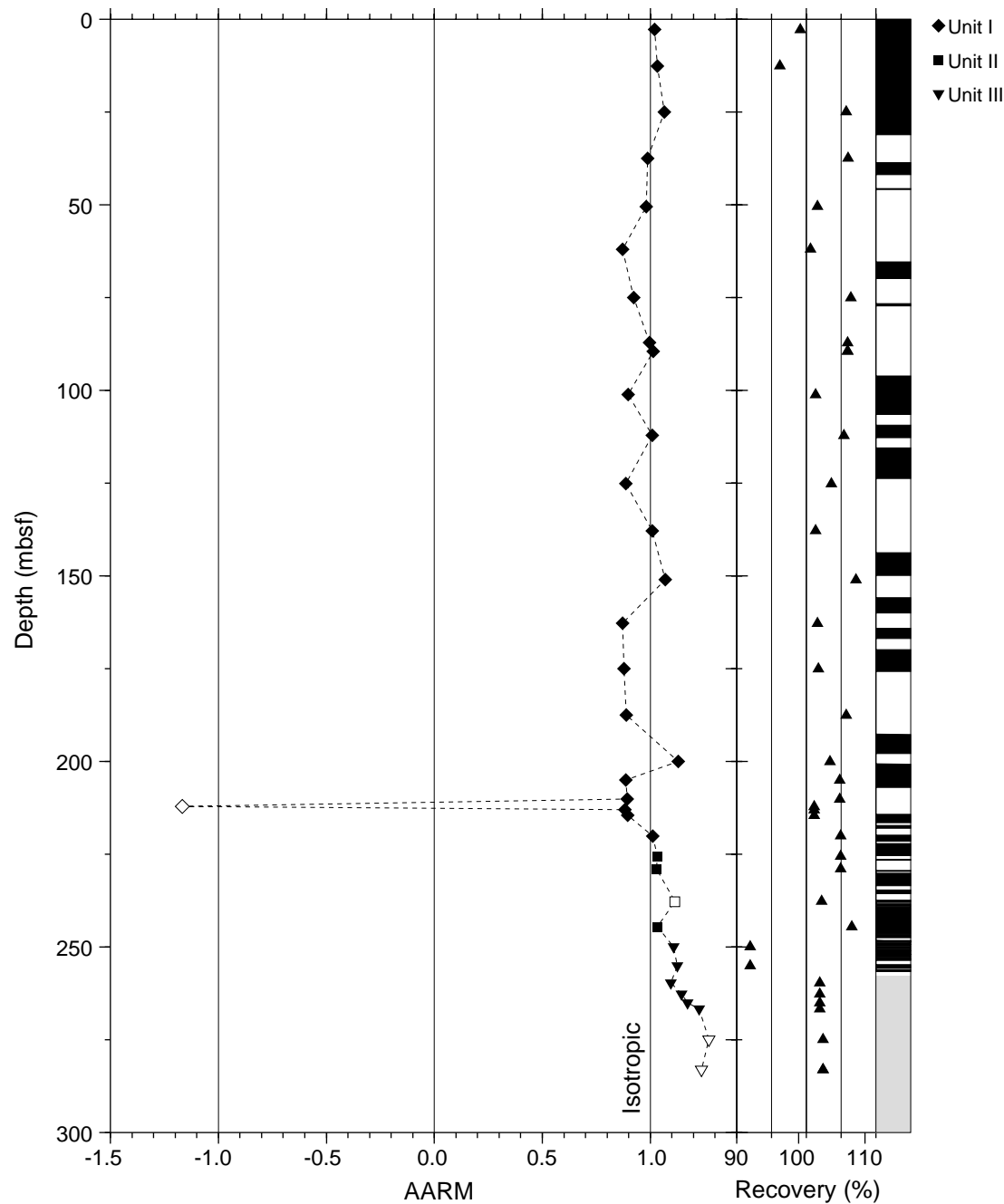


Figure F2. *F*-statistics for anisotropy vs. depth for samples listed in Table T3, p. 16. A. *F*-statistic for isotropy/anisotropy; the threshold value for anisotropy is 3.84. B. *F*-statistic (F_{12}) for prolate/triaxial AMS ellipsoids; the threshold value for a prolate or triaxial ellipsoid is 4.25. C. *F*-statistic (F_{23}) for oblate/triaxial AMS ellipsoids; the threshold value for an oblate or triaxial ellipsoid is 4.5. D. If both F_{12} and F_{23} are greater than 4.25, the AMS ellipsoid is triaxial; symbols to the right of the dashed line indicate triaxial AMS ellipsoids.

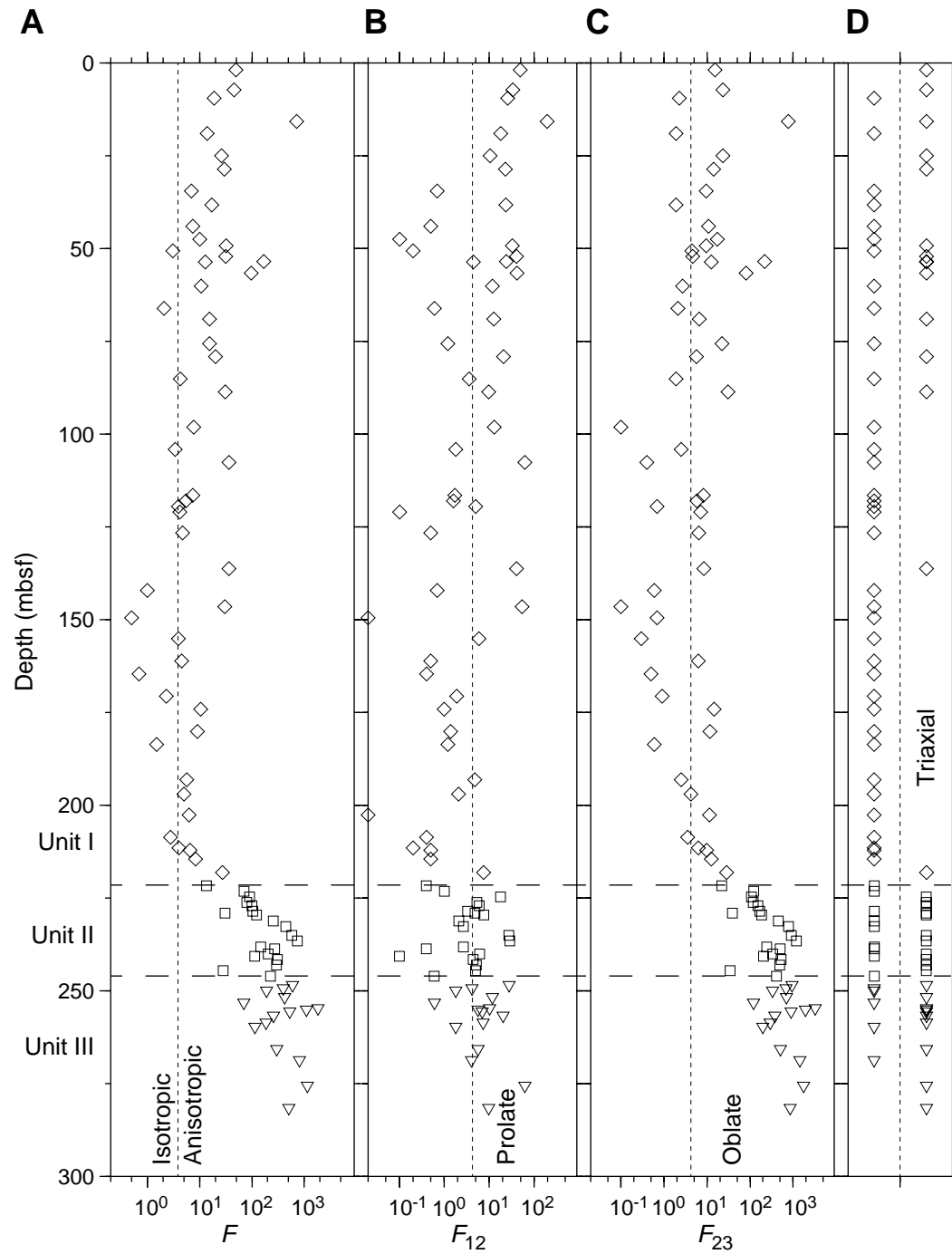


Figure F3. Principal axes of AMS ellipsoids. A. Unit I. B. Unit II. C. Unit III.

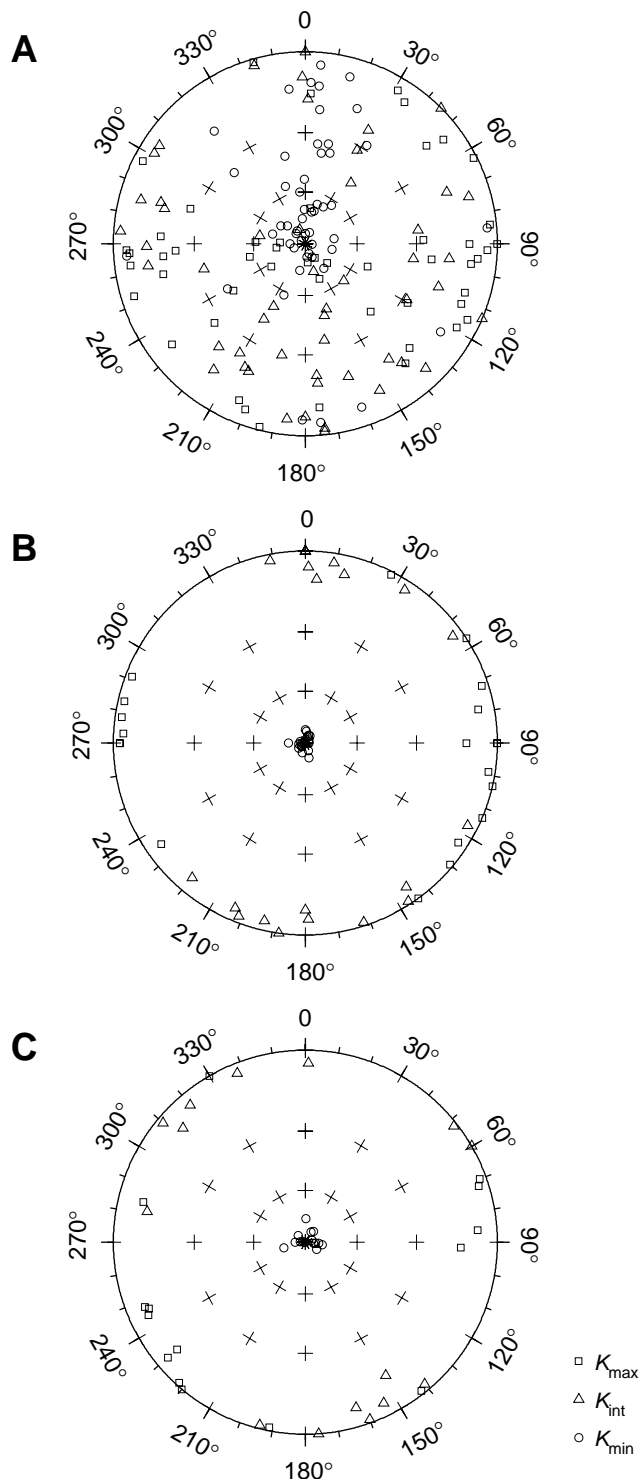


Figure F4. Variation in 95% confidence angles about the principal anisotropy axes vs. depth for samples listed in Table T3, p. 16. A. E_{12} , the 95% confidence angle between the K_{\max} and K_{int} anisotropy axes. B. E_{23} , the 95% confidence angle between the K_{int} and K_{\min} anisotropy axes. C. E_{31} , the 95% confidence angle between the K_{\min} and K_{\max} anisotropy axes.

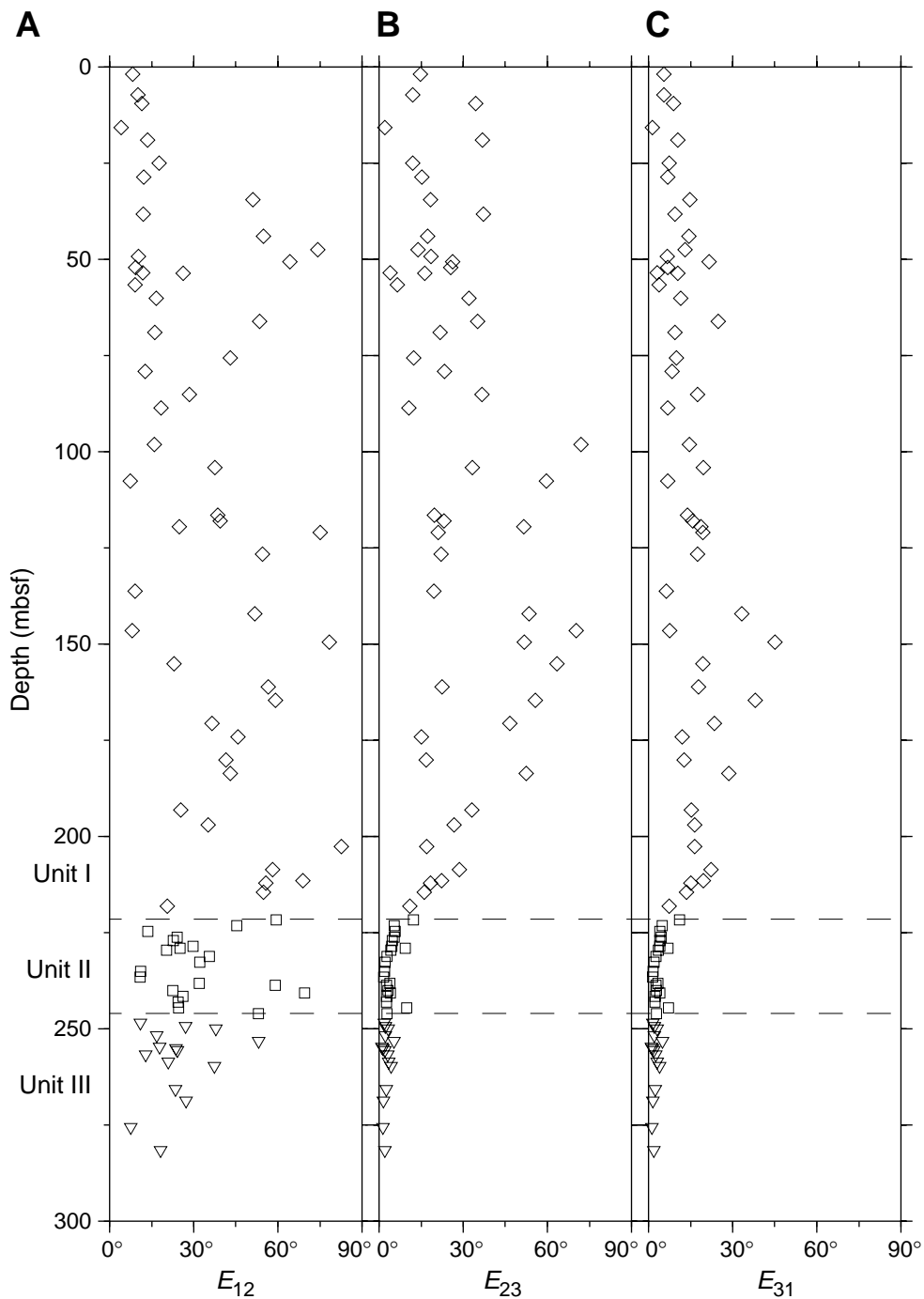


Figure F5. Principal axes of the triaxial AMS ellipsoid for Sample 191-1179B-1H-2, 38–40 cm. Black lines = 95% confidence ellipses for each axis.

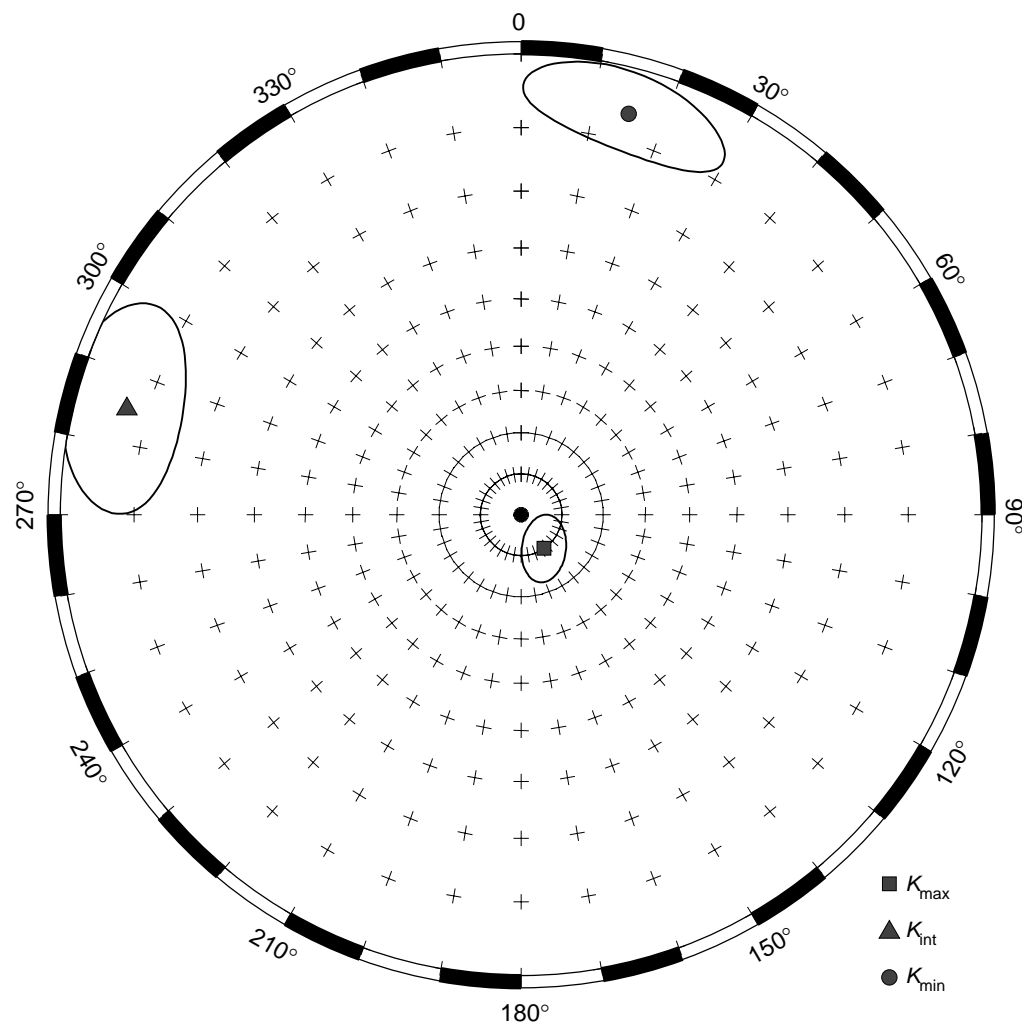


Figure F6. Anisotropy measures vs. depth for samples from Holes 1179B and 1179C. All parts of this figure use diamonds to show samples from sedimentary Unit I, squares to show samples from Unit II, and triangles to show samples from Unit III. A. Ellipsoid shape parameter T vs. depth; vertical dashed lines mark the boundaries for prolate and oblate AMS ellipsoids. Prolate ellipsoids are approximately cigar shaped, with K_{\max} inclination closest to 90°; oblate ellipsoids are approximately pancake shaped, with K_{\min} inclination closest to 90°. B. Ellipsoid shape parameter q vs. depth; vertical dashed line marks the boundary between oblate and prolate anisotropy of magnetic susceptibility ellipsoids. C–F. Anisotropy measures L , F , P , and P_i vs. depth; in all cases 1.0 is isotropic.

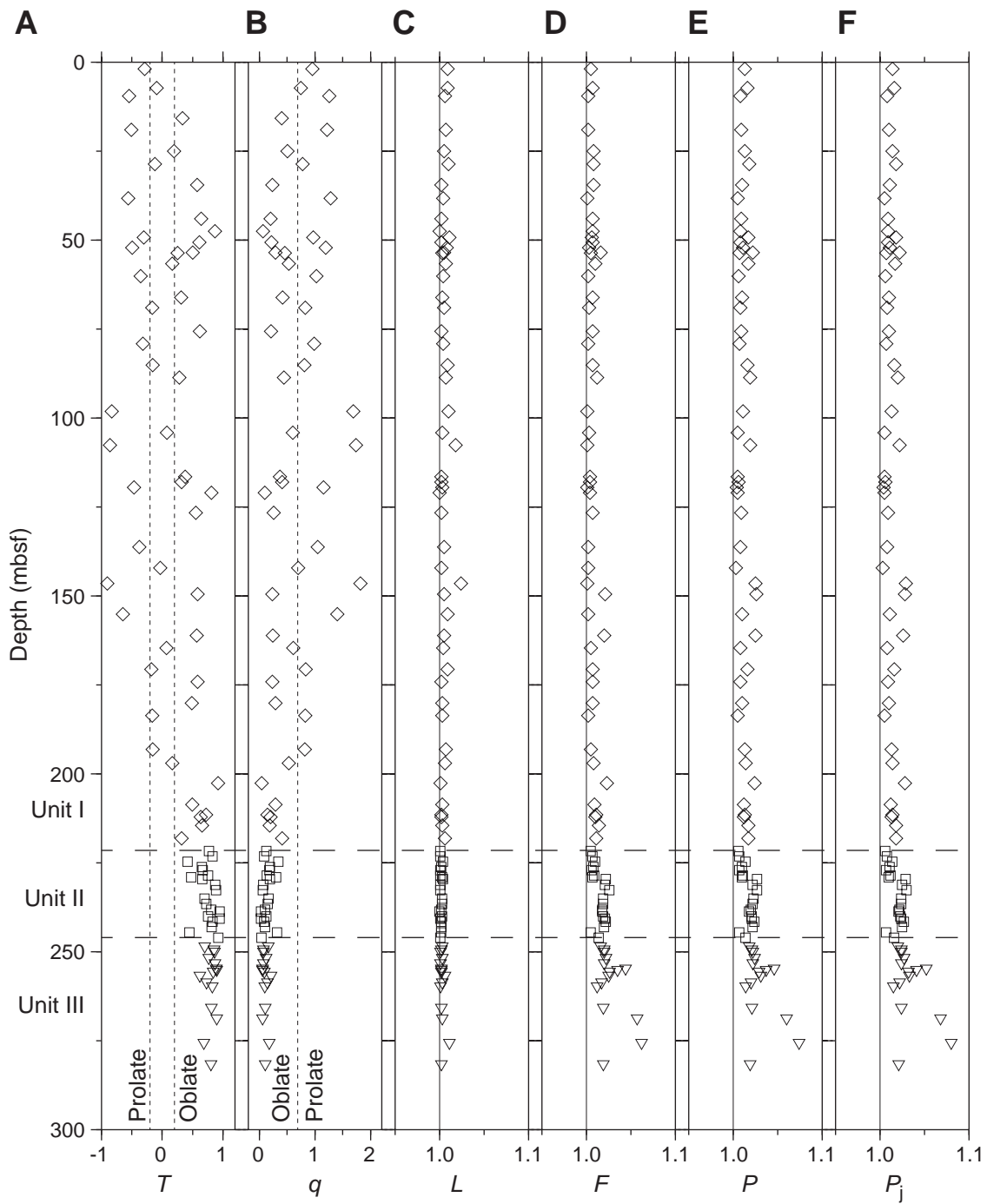


Table T1. Isothermal remanent magnetization (IRM) intensities (A/m), Hole 1179C. (See table notes. Continued on next page.)

Core, section, interval (cm)	Depth (mbsf)	Impulse field (mT)									
		25	50	75	100	200	300	400	500	750	1000
191-1179C-											
1H-1, 130–132	1.30	1.6281	2.7893	3.6636	4.3528	5.1696	5.3272	5.3767	5.4194	5.3997	5.3673
2H-1, 120–122	50.00	0.1120	0.1990	0.2773	0.3365	0.4512	0.5003	0.5244	0.5353	0.5475	0.5477
2H-2, 120–122	51.50	0.4871	0.9908	1.3128	1.5639	1.8136	1.8631	1.9012	1.9009	1.9117	1.9067
2H-3, 118–120	52.98	0.4151	0.7344	0.9843	1.1576	1.3570	1.4017	1.4253	1.4398	1.4487	1.4431
2H-4, 120–122	54.50	0.3877	0.8521	1.1937	1.4589	1.7637	1.8492	1.8926	1.9059	1.9321	1.9329
2H-5, 120–122	56.00	0.0901	0.1526	0.1991	0.2550	0.3374	0.3699	0.3847	0.3946	0.3997	0.4060
2H-6, 120–122	57.50	0.3085	0.6415	0.9488	1.0899	1.2762	1.3128	1.3319	1.3420	1.3519	1.3583
9H-1, 48–50	115.78	0.2323	0.4486	0.5917	0.7500	0.8951	0.9377	0.9612	0.9722	0.9610	0.9627
9H-2, 38–40	117.18	0.5711	1.2047	1.6866	2.0638	2.5027	2.6022	2.6617	2.6813	2.6751	2.6705
9H-3, 38–40	118.68	1.0562	2.1038	2.6250	3.1777	3.6724	3.7459	3.8100	3.8223	3.8041	3.7947
9H-4, 38–40	120.18	2.7897	5.4470	7.3225	9.1839	11.685	12.487	12.858	13.036	13.160	13.134
9H-5, 38–40	121.68	0.1914	0.3559	0.4854	0.5834	0.6913	0.7159	0.7147	0.7166	0.7332	0.7257
9H-6, 38–40	123.18	0.1698	0.3205	0.4039	0.4816	0.5595	0.5774	0.5778	0.5794	0.5927	0.5876
9H-7, 8–10	124.38	0.0362	0.0688	0.0967	0.1186	0.1525	0.1658	0.1668	0.1683	0.1761	0.1732
12H-1, 38–40*	144.18	0.1587	0.3031	0.4413	0.5279	0.5896	0.6097	0.6063	0.6096	0.6130	0.6030
12H-2, 38–40*	145.68	0.1753	0.2976	0.4986	0.6125	0.6980	0.7156	0.7224	0.7223	0.7253	0.7212
12H-3, 38–40*	147.18	0.1404	0.3115	0.4427	0.5419	0.6045	0.6156	0.6193	0.6185	0.6255	0.6267
12H-4, 38–40*	148.68	0.0845	0.1771	0.2471	0.2950	0.3275	0.3331	0.3355	0.3379	0.3383	0.3283
12H-5, 38–40*	150.18	0.1235	0.2088	0.2754	0.3164	0.3552	0.3635	0.3668	0.3698	0.3688	0.3655
12H-6, 38–40*	151.68	0.1689	0.2923	0.3790	0.4444	0.5021	0.5127	0.5180	0.5207	0.5222	0.5241
12H-7, 38–40*	153.18	0.0728	0.1374	0.1775	0.2142	0.2588	0.2722	0.2773	0.2808	0.2832	0.2842
19H-1, 38–40*	210.68	0.00689	0.01248	0.02042	0.02639	0.04176	0.04844	0.05122	0.05278	0.05388	0.05382
19H-2, 38–40*	212.18	0.00658	0.01560	0.02222	0.03005	0.04893	0.05736	0.06143	0.06312	0.06475	0.06509
19H-3, 38–40*	213.68	0.00935	0.01942	0.02955	0.03832	0.06379	0.07513	0.08094	0.08311	0.08576	0.08654
19H-4, 38–40*	215.18	0.00677	0.01826	0.02641	0.03602	0.05970	0.06975	0.07428	0.07618	0.07772	0.07800
19H-5, 38–40*	216.68	0.00866	0.02083	0.03320	0.04460	0.06853	0.07787	0.08255	0.08446	0.08633	0.08636
19H-6, 38–40*	218.18	0.09712	0.16867	0.23013	0.26388	0.31657	0.33591	0.34494	0.34659	0.35915	0.36592
19H-7, 38–40*	219.68	0.18510	0.37360	0.48346	0.56668	0.66558	0.69047	0.70614	0.71216	0.72668	0.73570
20H-7, 64–66	229.44	0.8464	2.3576	2.8083	2.9066	3.1049	3.1369	3.0762	3.1322	3.1398	3.2209
21H-1, 28–30	229.58	0.9346	1.4195	1.7860	2.0339	2.2609	2.3230	2.3415	2.3492	2.3447	2.3732
21H-1, 68–70	229.98	0.7059	1.3001	1.5717	1.7829	1.9879	2.0376	2.0591	2.0734	2.0842	2.1025
21H-1, 120–122	230.50	1.0384	1.8009	2.1884	2.4621	2.6972	2.7731	2.8050	2.8276	2.8445	2.8665
21H-2, 38–40	231.18	1.0793	2.1061	2.5898	2.9252	3.2990	3.4120	3.4642	3.4931	3.5168	3.5388
21H-2, 120–122	232.00	0.9458	1.6352	1.9667	2.2061	2.4433	2.5128	2.5481	2.5709	2.5928	2.6093
21H-3, 38–40	232.68	0.9146	1.6162	1.9347	2.1715	2.4366	2.5169	2.5577	2.5803	2.6039	2.6217
21H-3, 139–141	233.69	0.7783	1.6223	1.9477	2.2016	2.4585	2.5388	2.5809	2.6074	2.6388	2.6531
21H-4, 59–61	234.49	0.9495	1.7496	2.0813	2.3424	2.6015	2.6684	2.6707	2.6906	2.7132	2.7489
21H-4, 120–122	235.00	0.9833	1.6694	2.0299	2.3105	2.5462	2.6189	2.6404	2.6591	2.6879	2.7103
21H-5, 24–26	235.54	0.9212	1.7940	2.1858	2.4516	2.7130	2.8023	2.8308	2.8618	2.9163	2.9289
21H-5, 120–122	236.50	0.8051	1.6723	2.0166	2.1892	2.3963	2.4653	2.4944	2.5175	2.5563	2.5757
21H-6, 38–40	237.18	0.8250	1.5267	1.9173	2.1446	2.3422	2.4141	2.4502	2.4720	2.5068	2.5257
21H-6, 94–96	237.74	0.9585	1.5469	1.9229	2.0960	2.2704	2.3348	2.3676	2.3909	2.4213	2.4400
21H-6, 139–141	238.19	1.0161	1.7032	2.0299	2.2891	2.4958	2.5715	2.6144	2.6353	2.6730	2.6959
21H-7, 38–40	238.68	0.8959	3.1975	3.5316	3.5734	3.7541	3.7583	3.6935	3.7568	3.7462	3.8159
22H-1, 48–50	239.28	1.5916	2.8786	3.8537	4.5184	5.5844	5.9545	6.1149	6.1618	6.2634	6.2119
22H-1, 120–122	240.00	1.1973	1.9312	2.4741	2.7397	3.0358	3.1393	3.1907	3.1995	3.2395	3.2181
22H-2, 38–40	240.68	0.8357	1.7280	2.0281	2.2584	2.4842	2.5558	2.5914	2.6013	2.6348	2.6348
22H-2, 120–122	241.50	1.2323	2.0469	2.6382	2.9009	3.2348	3.3374	3.3872	3.4078	3.4464	3.4729
22H-3, 44–46	242.24	0.9821	1.5976	1.8734	2.0972	2.3084	2.3762	2.4145	2.4295	2.4582	2.4180
22H-3, 124–126	243.04	0.9728	1.9319	2.3100	2.5643	2.7967	2.8803	2.9277	2.9489	2.9842	2.9411
22H-4, 38–40	243.68	1.1645	2.3402	2.8303	3.1445	3.4768	3.5938	3.6595	3.6858	3.7401	3.7627
22H-6, 134–136	247.64	1.9544	5.3295	5.9540	5.9451	6.1547	6.1276	6.0528	6.1324	6.1099	6.2178
22H-7, 38–40	248.18	2.0039	6.2867	6.9371	6.8236	7.0269	6.9553	6.9099	6.9736	6.9257	7.0774
22H-7, 74–76	248.54	2.1387	7.1216	7.8263	7.6877	7.9073	7.8140	7.7379	7.8234	7.7520	7.9580
25X-4, 120–122	272.50	13.065	19.745	20.863	20.969	21.441	21.314	21.332	21.372	21.248	21.555
25X-CC, 19–21	272.97	13.017	17.314	18.484	18.603	19.140	19.204	19.397	19.464	19.359	19.463
26X-1, 38–40	274.08	8.1160	13.979	17.157	17.796	18.079	18.115	17.925	18.163	18.274	18.293
26X-1, 120–122	274.90	9.1263	17.325	19.815	20.357	20.255	20.233	19.873	20.157	20.039	19.879
26X-2, 38–40	275.58	10.771	17.931	20.059	20.605	20.693	20.749	20.400	20.715	20.600	20.480
26X-2, 120–122	276.40	9.4679	15.580	18.324	19.183	19.433	19.410	19.358	19.449	19.290	19.348
26X-3, 38–40	277.08	10.342	14.727	16.917	17.806	18.312	18.121	18.315	18.319	18.247	18.309
26X-3, 120–122	277.90	10.142	14.233	15.526	16.502	17.225	17.045	17.512	17.496	17.416	17.488
26X-4, 38–40	278.58	8.3235	12.812	13.529	14.154	14.763	14.821	15.001	14.947	15.014	15.066
26X-4, 120–122	279.40	7.9416	11.805	13.732	14.537	14.843	14.678	14.914	15.040	15.052	15.079
26X-5, 38–40	280.08	8.1981	12.790	14.788	15.571	15.920	15.794	15.991	16.115	15.362	13.415
26X-5, 120–122	280.90	11.168	17.878	19.474	19.548	19.751	19.654	19.671	19.697	19.623	19.774

Table T1 (continued).

Core, section, interval (cm)	Depth (mbsf)	Impulse field (mT)									
		25	50	75	100	200	300	400	500	750	1000
26X-6, 38–40	281.58	15.272	21.011	21.983	21.607	21.585	21.433	21.611	21.551	21.817	21.532
26X-6, 120–122	282.40	16.788	19.425	20.068	19.824	20.176	19.885	20.250	19.890	20.046	19.933
26X-7, 38–40	283.08	19.379	20.078	21.053	21.744	22.311	21.669	22.131	22.102	22.211	22.191
26X-CC, 10–12	283.29	18.598	21.804	25.532	27.896	28.382	28.130	28.455	28.377	28.354	28.645
191-1179C-											
25X-1, 14–16	266.94	5.1738	8.3396	10.063	10.425	10.573	10.737	10.588	10.678	10.845	10.728
25X-1, 120–122	268.00	8.0718	12.162	14.722	15.219	15.146	15.330	15.175	15.258	15.533	15.368
25X-2, 44–46	268.74	9.7463	13.014	14.987	15.294	15.055	15.230	15.310	15.351	15.352	15.498
25X-2, 120–122	269.50	6.2764	8.3045	9.2964	9.6201	9.3759	9.6600	9.7976	9.8420	9.9481	10.212
25X-3, 38–40	270.18	6.7476	9.4814	10.620	11.059	10.851	11.178	11.274	11.281	11.333	11.669
25X-3, 120–122	271.00	7.6003	10.462	11.995	12.591	12.452	12.807	12.868	12.894	13.172	13.469
25X-4, 38–40	271.68	8.2527	10.940	13.014	13.354	13.522	13.700	13.896	13.853	14.163	14.336

Notes: * = the sample tray was inserted backward, which offset the sample from the measurement point. The intensities are ~50% of the true values.

Table T2. Anisotropy of anhysteretic remanent magnetism, Holes 1179B and 1179C.

Core, section, interval (cm)	Depth (mbsf)	AARM	NRM _x	NRM _y	NRM _z	ARM _x	ARM _y	ARM _z
191-1179B-								
1H-2, 126–128	2.77	1.020	1.497E–09	–3.395E–09	4.852E–09	1.970E–06	1.971E–06	1.937E–06
2H-4, 51–53	12.61	1.033	–7.812E–09	2.055E–09	8.274E–09	7.251E–07	7.175E–07	7.095E–07
3H-6, 38–40	24.99	1.064	–5.943E–09	–3.285E–09	6.466E–09	6.987E–07	6.366E–07	6.384E–07
5H-1, 134–136	37.44	0.988	–2.884E–09	–1.933E–09	–1.195E–08	7.575E–07	7.536E–07	7.552E–07
6H-4, 38–40	50.49	0.980	1.088E–09	–1.333E–09	–3.694E–09	4.945E–07	4.962E–07	5.018E–07
191-1179C-								
3H-3, 67–69	61.97	0.871	6.203E–10	3.607E–10	–1.293E–09	8.161E–08	8.117E–08	9.160E–08
4H-5, 124–126	75.04	0.922	–3.217E–10	–2.458E–09	–6.548E–09	4.054E–07	4.048E–07	4.343E–07
6H-1, 38–40	87.18	0.997	–2.568E–10	–2.621E–09	1.644E–08	1.243E–06	1.236E–06	1.261E–06
6H-2, 116–118	89.48	1.012	–1.636E–09	–1.616E–09	–5.566E–10	7.660E–07	7.674E–07	7.584E–07
7H-4, 38–40	101.18	0.897	8.493E–12	–9.879E–10	2.561E–09	1.584E–07	1.581E–07	1.796E–07
8H-5, 38–40	112.18	1.010	1.502E–08	–5.745E–09	2.150E–08	1.890E–06	1.861E–06	1.874E–06
10H-1, 38–40	125.18	0.887	6.301E–10	2.667E–09	–5.327E–09	2.876E–07	2.893E–07	3.179E–07
11H-3, 54–56	137.84	1.010	–4.808E–09	–5.824E–10	1.257E–09	1.006E–06	9.953E–07	9.948E–07
12H-5, 120–122	151.00	1.070	–6.248E–10	8.136E–10	–5.853E–10	5.739E–07	5.776E–07	5.374E–07
13H-7, 61–63	162.81	0.872	–6.655E–10	–5.080E–10	–1.444E–09	4.128E–08	4.237E–08	4.718E–08
15H-2, 124–126	175.04	0.877	6.367E–10	7.298E–11	7.755E–10	6.303E–08	6.278E–08	7.208E–08
16H-4, 120–122	187.50	0.888	2.180E–10	4.049E–10	–2.929E–10	3.792E–08	3.816E–08	4.218E–08
17H-6, 124–126	200.04	1.129	–6.765E–10	2.421E–10	5.070E–11	1.115E–07	8.417E–08	8.689E–08
18H-3, 120–122	205.00	0.887	–5.953E–11	3.954E–10	–1.974E–11	2.760E–08	2.814E–08	3.120E–08
18H-7, 38–40	210.18	0.892	3.418E–10	4.379E–10	–6.486E–11	1.959E–08	2.018E–08	2.178E–08
19H-2, 38–40	212.18	–1.167*	1.121E–09	9.332E–10	1.864E–07	3.319E–08	3.326E–08	1.588E–07
19H-2, 120–122	213.00	0.882	–1.202E–10	5.719E–10	–9.165E–11	3.475E–08	3.590E–08	3.970E–08
19H-3, 120–122	214.50	0.894	3.242E–11	6.156E–10	1.607E–10	2.843E–08	2.923E–08	3.203E–08
20H-1, 28–30	220.08	1.011	1.373E–09	3.959E–10	–5.598E–09	2.425E–06	2.450E–06	2.404E–06
20H-4, 120–122	225.50	1.033	9.637E–09	5.409E–10	–8.212E–09	2.795E–06	2.817E–06	2.703E–06
20H-7, 19–21	228.99	1.028	3.166E–09	1.295E–09	–5.302E–09	2.699E–06	2.704E–06	2.620E–06
21H-6, 94–96	237.74	1.114*	1.965E–08	–1.209E–08	8.245E–07	3.356E–06	3.325E–06	3.820E–06
22H-4, 120–122	244.50	1.032	–2.629E–09	–5.306E–09	3.708E–09	3.937E–06	3.964E–06	3.837E–06
23H-2, 104–106	249.98	1.109	–2.360E–09	–5.690E–09	2.383E–09	7.373E–06	7.289E–06	6.618E–06
23H-6, 14–16	255.08	1.124	–1.064E–08	4.264E–09	6.500E–10	1.022E–05	1.023E–05	9.097E–06
24H-2, 38–40	259.68	1.094	–2.595E–09	–2.425E–09	–1.063E–08	1.162E–05	1.166E–05	1.063E–05
24H-4, 38–40	262.68	1.145	7.523E–08	–7.198E–09	7.720E–08	1.909E–05	1.910E–05	1.673E–05
24H-5, 120–122	265.00	1.172	8.227E–09	1.457E–08	–7.260E–09	1.638E–05	1.667E–05	1.408E–05
24H-CC, 29–31	266.72	1.227	–4.080E–09	–5.680E–10	–4.553E–09	1.657E–05	1.678E–05	1.359E–05
26X-1, 120–122	274.90	1.271*	2.042E–07	7.360E–09	4.072E–06	3.302E–05	3.325E–05	3.006E–05
26X-7, 38–40	283.08	1.237*	–6.043E–08	8.789E–08	2.420E–06	6.030E–05	6.000E–05	5.102E–05

Notes: AARM = anisotropy of anhysteretic remanent magnetization, NRM = natural remanent magnetization, ARM = anhysteretic remanent magnetization. * = Isothermal remanent magnetization to 1 T was done before AARM was determined.

Table T3. Anisotropy of magnetic susceptibility. (See table notes. Continued on next three pages.)

Core, section, interval (cm)	Depth (mbsf)	Tests for anisotropy			Principal directions of anisotropy axes (°)						95% confidence angles			Mean susceptibility (10^{-6} SI)
		F	F_{12}	F_{23}	K_{\max} Declination	K_{\max} Inclination	K_{\min} Declination	K_{\min} Inclination	K_{\min} Declination	K_{\min} Inclination	E_{12}	E_{23}	E_{31}	
191-1179B-														
1H-2, 38-40	1.89	49.4	49.8	15.3	146	80	285	7	15	6	8.3	14.8	5.4	21.65
1H-5, 124-126	7.25	45.4	33.4	23.5	158	68	286	14	21	16	10.1	12.0	5.5	4.40
2H-2, 40-42	9.51	18.9	25.7	2.3	273	75	70	14	161	6	11.5	34.4	8.9	55.10
2H-6, 58-60	15.70	720.7	194.4	770.0	203	7	113	0	21	83	4.2	2.1	1.4	53.70
3H-2, 40-42	19.01	13.9	18.1	1.9	267	5	175	18	11	71	13.6	36.8	10.4	2.51
3H-6, 38-40	24.99	26.5	10.5	23.4	173	79	274	2	5	11	17.6	12.0	7.3	15.88
4H-2, 50-52	28.61	29.4	22.9	14.2	97	23	209	42	347	40	12.2	15.3	6.9	3.82
4H-6, 38-40	34.47	6.9	0.7	9.7	267	22	134	59	6	20	51.1	18.3	14.7	4.43
5H-2, 58-60	38.19	17.0	23.5	1.9	8	69	175	21	266	4	12.0	37.2	9.4	14.28
5H-6, 34-36	43.96	7.4	0.5	10.9	131	73	262	11	354	12	54.9	17.3	14.4	5.59
6H-2, 44-46	47.56	10.0	0.1	17.6	344	1	74	7	249	83	74.3	13.8	13.0	5.22
6H-6, 38-40	53.49	167.7	24.2	217.5	107	8	207	50	10	39	11.8	4.0	3.0	17.21
191-1179C-														
2H-1, 48-50	49.28	32.2	33.1	9.5	97	8	192	29	354	60	10.2	18.5	6.7	3.56
2H-2, 38-40	50.68	3.1	0.2	4.4	229	26	136	6	34	63	64.2	26.2	21.6	2.75
2H-3, 38-40	52.18	31.5	40.8	4.7	88	27	280	63	181	5	9.2	25.5	6.9	5.93
2H-4, 38-40	53.68	12.9	4.4	12.5	257	57	98	31	2	10	26.2	16.3	10.4	17.23
2H-6, 38-40	56.68	96.4	41.4	81.2	263	5	169	36	359	53	9.1	6.5	3.8	5.16
3H-2, 38-40	60.18	10.8	11.9	2.7	236	66	29	22	123	10	16.7	32.1	11.5	5.46
3H-6, 38-40	66.18	2.1	0.6	2.1	135	15	45	0	315	75	53.4	35.2	24.8	2.59
4H-1, 122-124	69.02	15.4	12.8	6.6	111	8	204	18	358	70	16.1	21.8	9.5	4.10
4H-6, 28-30	75.58	15.4	1.2	22.3	136	38	256	33	13	34	43.1	12.3	10.0	4.96
5H-2, 38-40	79.18	20.1	21.1	5.7	63	1	153	9	327	81	12.7	23.4	8.4	13.51
5H-6, 38-40	85.18	4.3	3.6	1.9	92	3	1	16	192	74	28.5	36.6	17.4	2.03
6H-2, 38-40	88.68	30.7	9.7	30.6	268	4	359	8	153	81	18.3	10.6	6.8	2.69
7H-2, 38-40	98.18	7.7	13.1	0.1	273	16	165	48	15	38	15.9	72.0	14.6	2.81
7H-6, 38-40	104.18	3.4	1.8	2.5	272	61	83	29	175	4	37.5	33.3	19.5	16.33
8H-2, 38-40	107.68	36.5	63.2	0.4	140	12	37	47	240	40	7.4	59.7	6.9	3.43
9H-1, 120-122	116.50	7.4	1.7	8.3	2	14	269	11	143	72	38.6	19.7	13.9	4.48
9H-2, 120-122	118.00	5.5	1.6	5.8	287	26	162	51	32	28	39.5	23.2	15.7	3.70
9H-3, 120-122	119.50	3.9	5.0	0.7	110	52	216	12	315	35	24.8	51.6	18.7	3.16
9H-4, 120-122	121.00	4.2	0.1	7.1	51	12	144	17	287	70	75.1	21.1	19.3	2.67
10H-2, 38-40	126.68	4.7	0.5	6.5	120	27	220	20	341	55	54.5	22.1	17.4	2.11
11H-2, 48-50	136.28	36.6	41.1	8.5	263	73	96	16	5	4	9.1	19.5	6.3	5.34
11H-6, 38-40	142.18	1.0	0.7	0.6	31	4	301	5	160	84	51.7	53.5	33.2	3.40
12H-2, 120-122	146.50	30.3	53.9	0.1	265	17	174	1	80	73	8.0	70.3	7.6	1.30
12H-4, 120-122	149.50	0.5	0.0	0.7	175	9	338	81	85	3	78.3	51.7	45.1	1.98
13H-2, 38-40	155.18	3.9	5.9	0.3	119	6	211	23	17	66	23.0	63.4	19.3	1.70
13H-6, 38-40	161.18	4.5	0.5	6.3	233	8	141	13	353	75	56.6	22.4	17.9	0.68
14H-2, 38-40	164.68	0.7	0.4	0.5	237	42	119	28	7	35	59.2	55.7	38.0	1.41
14H-6, 38-40	170.68	2.3	1.9	0.9	115	4	206	19	15	70	36.5	46.7	23.5	1.21
15H-2, 38-40	174.18	10.4	1.0	14.8	53	6	163	73	321	16	45.7	15.0	12.0	2.12
15H-6, 38-40	180.18	9.1	1.4	11.6	258	16	162	18	26	66	41.5	16.8	12.7	3.39
16H-2, 38-40	183.68	1.5	1.2	0.6	297	3	29	32	203	58	43.0	52.5	28.6	4.06
17H-2, 38-40	193.18	5.7	4.8	2.5	35	6	304	5	173	82	25.3	33.0	15.3	2.62
17H-4, 120-122	197.00	5.0	2.1	4.2	95	6	186	5	318	82	35.2	26.8	16.4	2.12

Table T3 (continued).

Core, section, interval (cm)	Depth (mbsf)	Normed principal susceptibilities			Principal susceptibility uncertainty	Normed anisotropy tensor					Anisotropy factors						
		K _{max}	K _{int}	K _{min}		K _{xx}	K _{xy}	K _{xz}	K _{yy}	K _{yz}	K _{zz}	T	q	L	F	P	
191-1179B-																	
1H-2, 38-40	1.89	1.0073	0.9987	0.9940	0.0005	0.9945	-0.0013	-0.0016	0.9985	0.0007	1.0070	-0.287	0.949	1.009	1.005	1.013	1.014
1H-5, 124-126	7.25	1.0083	0.9995	0.9921	0.0007	0.9946	-0.0026	-0.0047	0.9988	0.0004	1.0066	-0.088	0.747	1.009	1.007	1.016	1.016
2H-2, 40-42	9.51	1.0046	0.9986	0.9968	0.0005	0.9970	0.0005	0.0003	0.9988	-0.0016	1.0042	-0.542	1.254	1.006	1.002	1.008	1.008
2H-6, 58-60	15.70	1.5563	1.1381	0.3056	0.0134	1.4787	0.1442	-0.133	1.1991	-0.0529	0.3222	0.331	0.402	1.368	3.724	5.092	5.626
3H-2, 40-42	19.01	1.0054	0.9984	0.9961	0.0007	0.9982	0.0004	-0.0007	1.0053	-0.0007	0.9964	-0.511	1.214	1.007	1.002	1.009	1.010
3H-6, 38-40	24.99	1.0063	1.0009	0.9929	0.0007	0.9934	-0.0007	-0.0025	1.0008	0.0000	1.0058	0.197	0.503	1.005	1.008	1.013	1.014
4H-2, 50-52	28.61	1.0093	0.9993	0.9914	0.0009	0.9950	0.0000	-0.0042	1.0074	0.0044	0.9976	-0.119	0.777	1.010	1.008	1.018	1.018
4H-6, 38-40	34.47	1.0041	1.0020	0.9939	0.0012	0.9949	-0.0006	-0.0026	1.0038	-0.001	1.0013	0.578	0.236	1.002	1.008	1.010	1.011
5H-2, 58-60	38.19	1.0028	0.9991	0.9981	0.0003	0.9996	0.0000	0.0013	0.9981	0.0003	1.0023	-0.562	1.281	1.004	1.001	1.005	1.005
5H-6, 34-36	43.96	1.0034	1.0019	0.9947	0.0010	0.9951	0.0006	-0.0018	1.0019	0.0005	1.0030	0.640	0.198	1.002	1.007	1.009	1.009
6H-2, 44-46	47.56	1.0027	1.0022	0.9950	0.0008	1.0027	-0.0002	0.0003	1.0022	0.0009	0.9951	0.870	0.067	1.000	1.007	1.008	1.009
6H-6, 38-40	53.49	1.0089	1.0035	0.9876	0.0005	0.9945	-0.0031	-0.0079	1.0080	-0.0006	0.9974	0.500	0.286	1.005	1.016	1.022	1.022
191-1179C-																	
2H-1, 48-50	49.28	1.0094	0.9983	0.9923	0.0009	0.9970	-0.0013	-0.0028	1.0090	0.0018	0.9940	-0.303	0.966	1.011	1.006	1.017	1.018
2H-2, 38-40	50.68	1.0032	1.0017	0.9951	0.0014	1.0013	0.0000	-0.0026	1.0020	-0.002	0.9967	0.616	0.213	1.002	1.007	1.008	1.009
2H-3, 38-40	52.18	1.0061	0.9983	0.9956	0.0005	0.9956	0.0002	0.0003	1.0045	0.0032	0.9998	-0.494	1.193	1.008	1.003	1.011	1.011
2H-4, 38-40	53.68	1.0034	1.0006	0.9960	0.0006	0.9962	0.0000	-0.001	1.0014	-0.0012	1.0024	0.255	0.458	1.003	1.005	1.007	1.007
2H-6, 38-40	56.68	1.0078	1.0009	0.9913	0.0005	0.9976	0.0009	-0.0047	1.0076	-0.0005	0.9948	0.167	0.526	1.007	1.010	1.017	1.017
3H-2, 38-40	60.18	1.0033	0.9993	0.9974	0.0005	0.9990	0.0011	-0.0007	0.9985	-0.0015	1.0026	-0.354	1.023	1.004	1.002	1.006	1.006
3H-6, 38-40	66.18	1.0044	1.0010	0.9945	0.0020	1.0024	-0.0014	-0.0017	1.0024	0.0017	0.9952	0.313	0.414	1.003	1.007	1.010	1.010
4H-1, 122-124	69.02	1.0042	0.9996	0.9962	0.0006	0.9998	-0.0015	-0.0013	1.0035	0.0007	0.9967	-0.164	0.821	1.005	1.003	1.008	1.008
4H-6, 28-30	75.58	1.0036	1.0019	0.9945	0.0007	0.9977	-0.0016	-0.004	1.0022	-0.0002	1.0002	0.621	0.209	1.002	1.007	1.010	1.010
5H-2, 38-40	79.18	1.0038	0.9993	0.9969	0.0004	1.0002	0.0090	-0.0003	1.0028	0.0003	0.9970	-0.317	0.981	1.004	1.002	1.007	1.007
5H-6, 38-40	85.18	1.0084	0.9992	0.9924	0.0022	0.9987	-0.0004	0.0018	1.0084	0.0009	0.9929	-0.155	0.812	1.009	1.007	1.016	1.016
6H-2, 38-40	88.68	1.0086	1.0018	0.9896	0.0010	1.0016	0.0003	0.0017	1.0085	-0.0013	0.9899	0.281	0.439	1.007	1.012	1.019	1.020
7H-2, 38-40	98.18	1.0073	0.9968	0.9959	0.0013	0.9963	-0.0006	-0.0003	1.0065	-0.0029	0.9972	-0.83	1.687	1.010	1.001	1.011	1.013
7H-6, 38-40	104.18	1.0027	1.0001	0.9972	0.0008	0.9972	0.0002	0.0002	1.0007	-0.0011	1.0020	0.077	0.600	1.003	1.003	1.005	1.005
8H-2, 38-40	107.68	1.0124	0.9945	0.9931	0.0010	1.0042	-0.0088	-0.0023	1.0011	0.0029	0.9946	-0.859	1.737	1.018	1.001	1.019	1.022
9H-1, 120-122	116.50	1.0022	1.0006	0.9971	0.0005	1.0019	0.0002	0.0012	1.0005	-0.0006	0.9975	0.379	0.367	1.002	1.004	1.005	1.005
9H-2, 120-122	118.00	1.0028	1.0007	0.9965	0.0008	0.9985	-0.0019	-0.0012	1.0014	-0.0017	1.0002	0.317	0.412	1.002	1.004	1.006	1.006
9H-3, 120-122	119.50	1.0023	0.9994	0.9983	0.0006	0.9992	0.0000	-0.0008	1.0000	0.0017	1.0008	-0.464	1.155	1.003	1.001	1.004	1.004
9H-4, 120-122	121.00	1.0016	1.0012	0.9971	0.0007	1.0013	0.0003	-0.0003	1.0010	0.0013	0.9977	0.814	0.098	1.000	1.004	1.005	1.005
10H-2, 38-40	126.68	1.0035	1.0016	0.9949	0.0012	1.0000	0.0000	-0.0034	1.0025	0.0017	0.9975	0.552	0.253	1.002	1.007	1.009	1.009
11H-2, 48-50	136.28	1.0044	0.9990	0.9966	0.0004	0.9966	-0.0002	-0.0003	0.9994	-0.0015	1.0040	-0.376	1.049	1.005	1.002	1.008	1.008
11H-6, 38-40	142.18	1.0017	1.0000	0.9983	0.0010	1.0012	0.0008	0.0003	1.0004	0.0000	0.9983	-0.033	0.696	1.002	1.003	1.003	1.003
12H-2, 120-122	146.50	1.0163	0.9924	0.9912	0.0015	0.9926	0.0021	-0.0007	1.0140	-0.0069	0.9933	-0.904	1.817	1.024	1.001	1.025	1.029
12H-4, 120-122	149.50	1.0104	1.0050	0.9845	0.0112	1.0101	-0.0023	-0.0009	0.9848	-0.0009	1.0051	0.584	0.232	1.005	1.021	1.026	1.028
13H-2, 38-40	155.18	1.0063	0.9978	0.9959	0.0016	0.9995	-0.0037	-0.001	1.0042	0.0005	0.9963	-0.649	1.403	1.009	1.002	1.010	1.011
13H-6, 38-40	161.18	1.0099	1.0047	0.9854	0.0034	1.0053	0.0026	-0.0053	1.0079	0.0000	0.9868	0.572	0.240	1.005	1.020	1.025	1.026
14H-2, 38-40	164.68	1.0041	1.0002	0.9957	0.0029	0.9979	0.0006	-0.0032	1.0017	-0.0019	1.0004	0.068	0.608	1.004	1.005	1.008	1.008
14H-6, 38-40	170.68	1.0083	0.9991	0.9926	0.0030	1.0000	-0.0037	-0.0022	1.0066	0.0000	0.9934	-0.179	0.835	1.009	1.007	1.016	1.016
15H-2, 38-40	174.18	1.0033	1.0016	0.9950	0.0008	0.9986	0.0038	-0.0013	1.0003	0.0013	1.0011	0.585	0.231	1.002	1.007	1.008	1.009
15H-6, 38-40	180.18	1.0041	1.0016	0.9943	0.0010	1.0007	0.0000	-0.0026	1.0036	-0.0018	0.9957	0.490	0.292	1.003	1.007	1.010	1.010
16H-2, 38-40	183.68	1.0025	0.9997	0.9978	0.0011	0.9999	-0.0013	0.0009	1.0018	0.0002	0.9983	-0.165	0.822	1.003	1.002	1.005	1.005
17H-2, 38-40	193.18	1.0067	0.9993	0.9940	0.0015	1.0041	0.0034	0.0014	1.0017	0.0003	0.9942	-0.158	0.815	1.007	1.005	1.013	1.013
17H-4, 120-122	197.00	1.0063	1.0007	0.9929	0.0017	1.0007	-0.0004	-0.0008	1.0062	0.0013	0.9931	0.165	0.527	1.006	1.008	1.014	1.014

Table T3 (continued).

Core, section, interval (cm)	Depth (mbsf)	Tests for anisotropy			Principal directions of anisotropy axes (°)						95% confidence angles			Mean susceptibility (10^{-6} SI)
		F	F_{12}	F_{23}	K_{\max} Declination	K_{\max} Inclination	K_{int} Declination	K_{int} Inclination	K_{\min} Declination	K_{\min} Inclination	E_{12}	E_{23}	E_{31}	
18H-2, 38–40	202.68	6.3	0.0	11.4	200	5	108	18	306	72	82.6	17.0	16.4	0.65
18H-6, 38–40	208.68	2.8	0.4	3.6	253	4	344	2	95	86	58.1	28.6	22.2	2.21
19H-1, 120–122	211.50	4.0	0.2	6.3	194	1	284	16	102	74	68.9	22.3	19.5	1.53
19H-2, 38–40	212.18	6.6	0.5	9.8	90	9	0	0	270	81	55.7	18.3	15.1	1.43
19H-3, 120–122	214.50	8.4	0.5	12.6	90	0	180	6	0	84	54.8	16.2	13.6	1.20
19H-6, 38–40	218.18	27.2	7.5	28.7	84	2	174	2	308	87	20.6	10.9	7.3	2.98
20H-2, 38–40	221.68	13.6	0.4	22.3	103	0	13	6	198	84	59.5	12.3	11.0	5.89
20H-3, 38–40	223.18	71.0	1.0	121.3	273	3	4	9	167	81	45.4	5.4	4.9	13.88
20H-4, 38–40	224.68	90.9	18.0	108.0	270	2	179	5	23	85	13.7	5.7	4.0	5.43
20H-5, 38–40	226.18	79.9	5.3	119.4	90	0	0	0	0	90	24.1	5.4	4.5	16.59
20H-5, 120–122	227.00	100.4	6.0	151.9	90	10	0	0	270	80	22.8	4.8	4.0	23.71
20H-6, 120–122	228.50	103.8	3.3	167.9	235	5	145	5	6	83	29.7	4.6	4.0	18.39
20H-7, 19–21	228.99	30.9	4.8	39.5	123	3	33	3	262	86	25.1	9.3	6.9	18.45
21H-1, 28–30	229.58	122.4	7.7	184.1	278	2	188	0	88	88	20.4	4.3	3.6	17.44
21H-2, 38–40	231.18	257.8	2.1	450.6	27	1	117	3	285	87	35.6	2.8	2.6	48.58
21H-3, 28–30	232.68	441.7	2.7	779.4	283	2	193	3	49	87	32.1	2.1	2.0	19.07
21H-4, 120–122	235.00	580.5	27.9	901.8	99	2	9	3	227	87	11.1	2.0	1.7	19.17
21H-5, 120–122	236.50	747.5	28.9	1186.4	57	0	147	1	317	89	10.9	1.7	1.5	18.64
21H-6, 139–141	238.19	146.2	2.7	245.4	72	2	162	1	272	88	32.0	3.8	3.4	19.15
21H-7, 38–40	238.68	274.9	0.4	501.7	113	0	203	4	19	86	59.0	2.6	2.6	17.59
22H-1, 120–122	240.00	206.4	6.2	334.9	130	1	220	5	33	85	22.5	3.2	2.8	21.93
22H-2, 38–40	240.68	112.2	0.1	204.9	291	2	201	2	63	88	69.6	4.1	4.0	18.38
22H-2, 120–122	241.50	308.3	4.4	525.5	79	5	349	2	234	85	26.1	2.6	2.4	48.44
22H-3, 124–126	243.04	293.7	5.2	495.1	144	0	54	3	239	87	24.4	2.7	2.4	21.59
22H-4, 120–122	244.50	28.1	5.0	34.9	270	2	1	5	160	85	24.7	9.9	7.2	64.54
22H-5, 120–122	246.00	226.2	0.6	407.8	90	0	180	8	0	82	53.0	2.9	2.8	55.94
23H-1, 14–16	248.44	600.3	28.1	934.3	330	0	60	0	0	90	11.0	1.9	1.6	86.46
23H-2, 36–38	249.30	393.0	4.1	679.5	222	1	313	8	122	82	27.0	2.3	2.1	92.22
23H-2, 104–106	249.98	189.4	1.8	329.5	220	0	310	2	73	86	37.9	3.3	3.0	83.78
23H-3, 120–122	251.64	423.0	11.7	691.9	230	4	320	4	97	85	16.8	2.2	2.0	103.84
23H-4, 127–129	253.21	69.9	0.6	121.8	284	8	194	1	95	82	53.2	5.3	5.0	312.45
23H-5, 120–122	254.64	1849.5	10.3	3274.4	248	6	338	3	95	84	17.8	1.0	1.0	924.75
23H-6, 14–16	255.08	1095.3	5.6	1944.2	230	8	140	2	36	82	23.6	1.3	1.3	327.15
23H-6, 64–66	255.58	523.0	7.0	894.8	245	6	154	4	28	83	24.1	2.0	1.8	376.30
23H-7, 30–32	256.74	256.5	20.6	372.3	191	1	281	10	98	80	12.8	3.1	2.5	369.90
24H-1, 79–81	258.59	184.7	7.3	292.7	70	2	160	1	273	87	20.9	3.5	3.0	309.65
24H-2, 38–40	259.68	115.2	1.8	195.2	142	1	52	1	267	89	37.3	4.2	3.9	306.65
24H-6, 38–40	265.68	300.2	5.6	503.7	247	7	149	12	1	76	23.5	2.6	2.4	322.25
25X-2, 44–46	268.74	804.8	4.0	1429.2	86	6	176	0	270	84	27.2	1.6	1.5	1614.00
26X-2, 38–40	275.58	1151.3	62.2	1765.1	92	12	1	4	255	77	7.5	1.4	1.2	2278.00
26X-6, 38–40	281.58	508.7	9.8	852.3	72	3	163	6	313	84	18.2	2.0	1.8	1735.00

Notes: F = F -test for anisotropy/isotropy at the 95% significance level; values > 3.48 are anisotropic. F_{12} = F -test for triaxial/rotational prolate, F_{23} = F -test for triaxial/rotational oblate ellipsoids; if values of both F_{12} and F_{23} are > 4.25 , ellipsoid is triaxial. E_{12} = 95% confidence angle in degrees between the K_{\max} and K_{int} principal directions, E_{23} = 95% confidence angle in degrees between the K_{int} and K_{\min} principal directions, E_{31} = 95% confidence angle in degrees between the K_{\min} and K_{\max} principal directions. A 95% confidence ellipse for K_{\max} can be constructed using E_{12} and E_{31} as the major and minor axes of the ellipse. Figure F2, p. 8, shows the 95% confidence ellipses of K_{\max} , K_{int} and K_{\min} for Sample 191-1179B-1H-2, 38–40 cm. Normed principal susceptibilities = susceptibilities along the K_{\max} , K_{int} , and K_{\min} principal directions divided by the mean susceptibility. The uncertainty in the principal susceptibilities is based on the error in fitting the susceptibility tensor to the measured susceptibilities. The anisotropy factors are calculated from the principal normed susceptibilities ($K_{\max} > K_{\text{int}} > K_{\min}$) and their respective natural logarithms (n_{\max} , n_{int} , and n_{\min}). $T = (2n_{\text{int}} - n_{\max} - n_{\min})/(n_{\max} - n_{\min})$. $q = (K_{\max} - K_{\text{int}})/[(K_{\max} + K_{\text{int}})/2 - K_{\min}]$. $L = K_{\max}/K_{\text{int}}$. $F = K_{\text{int}}/K_{\min}$. $P = K_{\max}/K_{\min}$. $P_j = \exp\{\sqrt{2(n_{\max} - n)^2 + (n_{\text{int}} - n)^2 + (n_{\min} - n)^2}\}$, where $n = (n_{\max} + n_{\text{int}} + n_{\min})/3$.

Table T3 (continued).

Core, section, interval (cm)	Depth (mbsf)	Normed principal susceptibilities			Principal susceptibility uncertainty	Normed anisotropy tensor					Anisotropy factors						
		K _{max}	K _{int}	K _{min}		K _{xx}	K _{xy}	K _{xz}	K _{yy}	K _{yz}	K _{zz}	T	q	L	F	P	P _j
18H-2, 38–40	202.68	1.0083	1.0074	0.9844	0.0030	1.0074	0.0014	-0.0041	1.0060	0.0055	0.9867	0.924	0.039	1.001	1.023	1.024	1.028
18H-6, 38–40	208.68	1.0049	1.0019	0.9932	0.0021	1.0022	0.0008	0.0000	1.0046	-0.0008	0.9933	0.493	0.290	1.003	1.009	1.012	1.012
19H-1, 120–122	211.50	1.0048	1.0031	0.9921	0.0019	1.0047	0.0006	0.0006	1.0023	-0.0029	0.9930	0.727	0.147	1.002	1.011	1.013	1.014
19H-2, 38–40	212.18	1.0047	1.0025	0.9928	0.0014	1.0025	0.0000	0.0000	1.0044	0.0019	0.9931	0.632	0.202	1.002	1.010	1.012	1.013
19H-3, 120–122	214.50	1.0065	1.0036	0.9899	0.0017	1.0035	0.0000	-0.0015	1.0065	0.0000	0.9900	0.660	0.186	1.003	1.014	1.017	1.018
19H-6, 38–40	218.18	1.0077	1.0018	0.9905	0.0009	1.0019	0.0006	-0.0003	1.0076	0.0006	0.9905	0.322	0.408	1.006	1.011	1.017	1.018
20H-2, 38–40	221.68	1.0021	1.0014	0.9965	0.0005	1.0014	-0.0002	0.0005	1.0020	0.0002	0.9966	0.772	0.121	1.001	1.005	1.006	1.006
20H-3, 38–40	223.18	1.0027	1.0020	0.9953	0.0003	1.0019	0.0000	0.0010	1.0027	-0.0003	0.9955	0.831	0.088	1.001	1.007	1.007	1.008
20H-4, 38–40	224.68	1.0058	1.0019	0.9923	0.0004	1.0018	0.0000	-0.0008	1.0058	-0.0005	0.9924	0.420	0.339	1.004	1.010	1.014	1.014
20H-5, 38–40	226.18	1.0039	1.0022	0.9940	0.0003	1.0022	0.0000	0.0000	1.0039	0.0000	0.9940	0.652	0.190	1.002	1.008	1.010	1.011
20H-5, 120–122	227.00	1.0026	1.0015	0.9959	0.0002	1.0015	0.0000	0.0000	1.0024	0.0012	0.9961	0.667	0.181	1.001	1.006	1.007	1.007
20H-6, 120–122	228.50	1.0039	1.0026	0.9934	0.0003	1.0029	0.0006	-0.0012	1.0035	-0.0002	0.9936	0.755	0.130	1.001	1.009	1.011	1.012
20H-7, 19–21	228.99	1.0041	1.0016	0.9943	0.0005	1.0023	-0.0012	0.0000	1.0033	0.0006	0.9944	0.481	0.298	1.003	1.007	1.010	1.010
21H-1, 28–30	229.58	1.0104	1.0059	0.9838	0.0007	1.0059	-0.0006	0.0000	1.0102	-0.001	0.9838	0.661	0.185	1.004	1.022	1.027	1.029
21H-2, 38–40	231.18	1.0078	1.0064	0.9857	0.0004	1.0075	0.0006	-0.0003	1.0067	0.0012	0.9858	0.873	0.066	1.001	1.021	1.022	1.025
21H-3, 28–30	232.68	1.0094	1.0079	0.9828	0.0004	1.0079	-0.0004	-0.0009	1.0092	-0.0011	0.9828	0.889	0.057	1.001	1.026	1.027	1.030
21H-4, 120–122	235.00	1.0086	1.0052	0.9862	0.0003	1.0053	-0.0006	0.0007	1.0084	0.0009	0.9863	0.701	0.162	1.003	1.019	1.023	1.024
21H-5, 120–122	236.50	1.0082	1.0053	0.9866	0.0002	1.0061	0.0013	-0.0002	1.0073	0.0002	0.9866	0.730	0.145	1.003	1.019	1.022	1.024
21H-6, 139–141	238.19	1.0072	1.0054	0.9874	0.0005	1.0055	0.0006	0.0000	1.0070	0.0007	0.9874	0.810	0.100	1.002	1.018	1.020	1.022
21H-7, 38–40	238.68	1.0061	1.0056	0.9883	0.0003	1.0056	-0.0002	-0.0012	1.0060	-0.0004	0.9884	0.946	0.027	1.000	1.018	1.018	1.021
22H-1, 120–122	240.00	1.0079	1.0053	0.9868	0.0005	1.0063	-0.0013	-0.0013	1.0068	-0.0008	0.9869	0.760	0.128	1.003	1.019	1.021	1.023
22H-2, 38–40	240.68	1.0072	1.0066	0.9862	0.0006	1.0067	-0.0002	-0.0004	1.0071	-0.0008	0.9863	0.948	0.026	1.001	1.021	1.021	1.024
22H-2, 120–122	241.50	1.0086	1.0066	0.9849	0.0004	1.0066	0.0003	0.0012	1.0084	0.0018	0.9851	0.832	0.088	1.002	1.022	1.024	1.027
22H-3, 124–126	243.04	1.0080	1.0060	0.9860	0.0004	1.0073	-0.001	0.0005	1.0067	0.0008	0.9860	0.815	0.097	1.002	1.020	1.022	1.025
22H-4, 120–122	244.50	1.0030	1.0011	0.9959	0.0004	1.0010	0.0000	0.0004	1.0030	-0.0002	0.9959	0.450	0.319	1.002	1.005	1.007	1.007
22H-5, 120–122	246.00	1.0049	1.0044	0.9907	0.0003	1.0042	0.0000	-0.0018	1.0049	0.0000	0.9909	0.926	0.038	1.001	1.014	1.014	1.016
23H-1, 14–16	248.44	1.0069	1.0042	0.9889	0.0002	1.0062	-0.0012	0.0000	1.0049	0.0000	0.9889	0.704	0.160	1.003	1.016	1.018	1.020
23H-2, 36–38	249.30	1.0076	1.0060	0.9864	0.0003	1.0068	0.0009	0.0014	1.0065	-0.0023	0.9868	0.856	0.075	1.002	1.020	1.021	1.024
23H-2, 104–106	249.98	1.0076	1.0062	0.9862	0.0005	1.0070	0.0007	-0.0005	1.0067	-0.0015	0.9864	0.864	0.071	1.001	1.020	1.022	1.024
23H-3, 120–122	251.64	1.0089	1.0061	0.9849	0.0004	1.0073	0.0014	0.0001	1.0076	-0.0021	0.9851	0.770	0.122	1.003	1.022	1.024	1.027
23H-4, 127–129	253.21	1.0076	1.0062	0.9862	0.0008	1.0063	-0.0003	0.0003	1.0071	-0.0029	0.9866	0.869	0.068	1.001	1.020	1.022	1.024
23H-5, 120–122	254.64	1.0158	1.0134	0.9708	0.0003	1.0137	0.0009	0.0003	1.0149	-0.0049	0.9714	0.894	0.055	1.002	1.044	1.046	1.052
23H-6, 14–16	255.08	1.0126	1.0107	0.9767	0.0003	1.0010	0.0005	-0.0041	1.0116	-0.003	0.9774	0.899	0.052	1.002	1.035	1.037	1.041
23H-6, 64–66	255.58	1.0102	1.0079	0.9820	0.0004	1.0080	0.0007	-0.0028	1.0096	-0.0017	0.9824	0.838	0.084	1.002	1.026	1.029	1.032
23H-7, 30–32	256.74	1.0121	1.0063	0.9817	0.0006	1.0118	0.0012	0.0005	1.0058	-0.0041	0.9824	0.619	0.211	1.006	1.025	1.031	1.033
24H-1, 79–81	258.59	1.0075	1.0048	0.9878	0.0004	1.0051	0.0009	0.0000	1.0071	0.0009	0.9878	0.727	0.146	1.003	1.017	1.020	1.022
24H-2, 38–40	259.68	1.0049	1.0037	0.9914	0.0004	1.0045	-0.0006	0.0000	1.0042	0.0003	0.9914	0.823	0.092	1.001	1.012	1.014	1.015
24H-6, 38–40	265.68	1.0077	1.0057	0.9866	0.0004	1.0050	0.0008	-0.0047	1.0072	-0.0003	0.9878	0.809	0.100	1.002	1.019	1.021	1.024
25X-2, 44–46	268.74	1.0202	1.0173	0.9624	0.0006	1.0173	0.0002	0.0000	1.0195	0.0062	0.9631	0.899	0.052	1.003	1.057	1.060	1.068
26X-2, 38–40	275.58	1.0272	1.0161	0.9567	0.0006	1.0159	-0.0011	0.0033	1.0240	0.0146	0.9601	0.684	0.172	1.011	1.062	1.074	1.080
26X-6, 38–40	281.58	1.0067	1.0049	0.9883	0.0003	1.0050	0.0006	-0.0012	1.0065	0.0014	0.9885	0.806	0.102	1.002	1.019	1.019	1.021